Age and Paleomagnetic Orientation of Diabase Intrusions, Coalsack Bluff, Antarctica

Senior Thesis

Winter, 1971

John E. Umstead

In cooperation with

Dr. R. Fleck

Dr. D. Elliot

Accepted

R. J. Fleck

Introduction

Coalsack Bluff, Antarctica (Fig. 1), has recently become an important fossil vertebrate locality. Stratigraphic work (Elliot, 1970, Elliot and Collinson, 1971, Barrett, 1969-1970) in the area has indicated a warm paleoclimate and a possible land link with South Africa and South America. From the paleomagnetic measurements of Dr. Alan Nairn of Case Western Reserve, three paleogeomagnetic poles were calculated in this paper. Age determinations made by this writer indicate two, probably separate, dolerite intrusions into the southern end of the bluff. Comparison of the dates with the pole positions indicates a rather rapid meridianal drift of the Antarctic continent toward its present location that is consistent with most models of Antarctica's drift pattern.

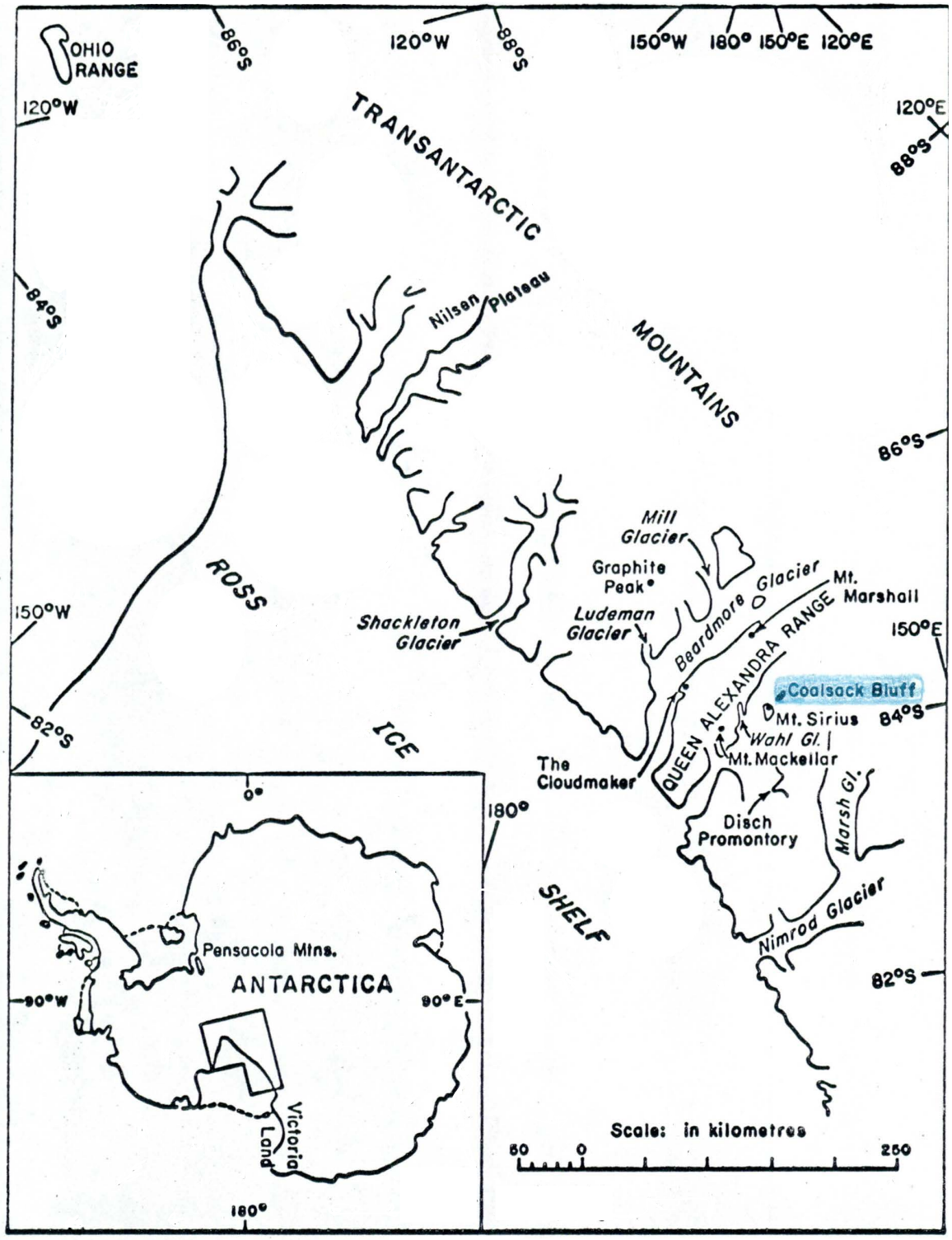
OHIO RANGE
86°S
120°W
88°S
150°W
180°
150°E
120°E
120°W
120°E
88°S
TRANSANTARCTIC
MOUNTAINS
84°S
Nilsen Plateau
86°S
Mill Glacier
Graphite Peak
Beardmore Glacier
Mt. Marshall
ROSS
150°W
Shackleton Glacier
Ludeman Glacier
150°E
QUEEN ALEXANDRA RANGE
Coalsack Bluff
Mt. Sirius
84°S
Wahl Gl.
Mt. Mackellar
82°S
ICE
The Cloudmaker
Marsh Gl.
Disch Promontory
180°
SHELF
Nimrod Glacier
82°S
0°
Pensacola Mtns.
ANTARCTICA
90°W
90°E
Victoria Land
180°
Scale: in kilometres
50
0
250

Figure 1

Stratigraphy

On Coalsack Bluff (Fig. 1) about 500 meters of probable Upper Permian and Lower Triassic sedimentary rocks are exposed (Fig. 2). These rocks are part of a sequence loosely termed Beacon. This term refers to nearly horizontal strata, mostly sandstone, of Devonian to Triassic age that unconformably overlie a Precambrian-Lower Paleozoic basement complex.

Buckley Formation

The upper 220 meters of the Permian Buckley Formation are exposed on Coalsack Bluff. It consists mainly of carbonaceous shale with lesser amounts of mudstone, sandstone, siltstone, and coal, arranged in cyclic sequences whose grain size decreases upward. The coarse part of each cycle is a medium-grained cross-bedded sandstone. A well-preserved Glossopteris flora occurs in the mudstone parts of each sequence. The environment suggestd is one of "deposition on a slowly subsiding flood plain with ephemeral lakes and swamps and meandering streams that flowed generally to the east and south" (Barrett, 1969, p. 47). The Buckley Formation has been assigned to the Permian on the basis of the Glossopteris Flora (Grindley, 1963, Barrett, 1969). Middle to Upper Permian conchostracans occur in a lithologically similar unit, the Mount Glossopteris Formation, in the Ohio Range 475 miles southeast (Doumani,and Tasch, 1965).

Fremouw Formation

On Coalsack Bluff approximately the lower 270 meters of the Fremouw Formation are exposed. In its lower portion this formation consists of a series of cyclic sequences whose grain size decreases upward. The cycles consist of channel sandstones and conglomeratic lenses and over-bank siltstones deposited on an alluvial plane by low sinuosity high gradient streams flowing northeast to east-northeast. The upper portion of this formation consists of fine-to-medium grained sandstone. A mammal-like reptile typical of the Lower Triassic of South Africa, Lystrosaurus, is among abundant disarticulated vertebrate fossils, few of which are skull fragments, from the conglomeratic lenses at the base of the

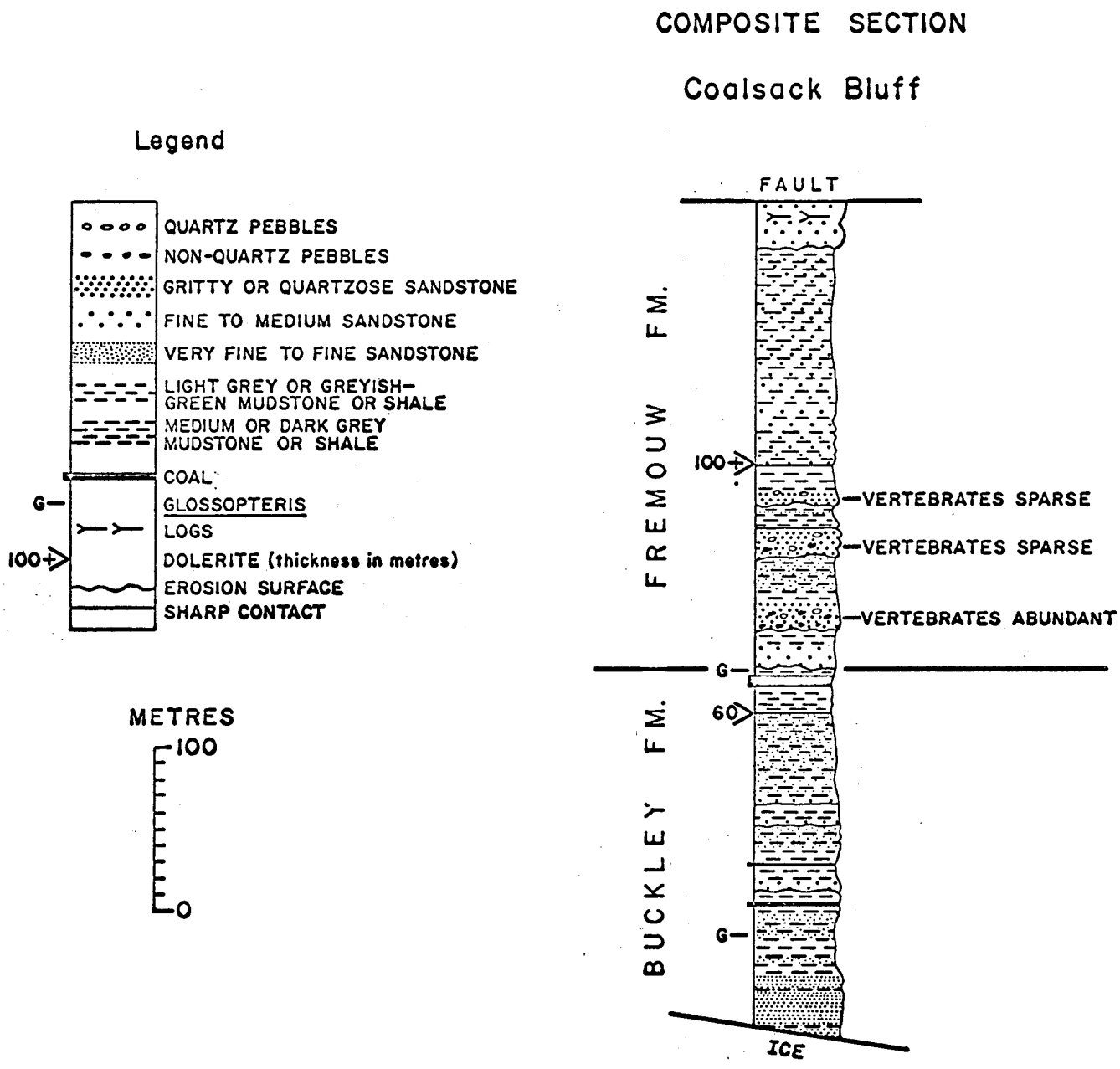
COMPOSITE SECTION
Coalsack Bluff
Legend
QUARTZ PEBBLES
NON-QUARTZ PEBBLES
GRITTY OR QUARTZOSE SANDSTONE
FINE TO MEDIUM SANDSTONE
VERY FINE TO FINE SANDSTONE
LIGHT GREY OR GREYISH-GREEN MUDSTONE OR SHALE
MEDIUM OR DARK GREY MUDSTONE OR SHALE
COAL
G
GLOSSOPTERIS
LOGS
100
DOLERITE (thickness in metres)
EROSION SURFACE
SHARP CONTACT
METRES
100
0
FAULT
FREMOUW FM.
100
VERTEBRATES SPARSE
VERTEBRATES SPARSE
VERTEBRATES ABUNDANT
G
BUCKLEY FM.
60
G
ICE

Figure 2

lower portion of the formation. The Fremouw has been assigned to the Lower Triassic on this basis.

Dolerite Sills

Two major discordant sills and one large intrusive mass are exposed on the southern end of Coalsack Bluff. These rocks have been assigned to the Ferrar Dolerite, the term applied to the Jurassic intrusions in Antarctica. McDougal, 1963, has K-Ar dates on the Ferrar of 153 million years at Mt. Markham, 93 miles to the north, and of 155 and 147 million years at Mt. Miller, 65 miles to the northeast. Wade and others, 1965, have K-Ar dates of 160-183 million years from the Shackleton Glacier area, 140 miles to the east. Depending on the age of the Triassic-Jurassic boundary, analyses reported in this paper indicate an Early to Middle Jurassic age for the intrusions with two, probably separate, phases occurring at about 178 and 167 million years ago.

Structure

At the southern end of Coalsack Bluff (Fig. 3), strata on the east side are gently dipping, but have steep dips on the west side. A north-south trending fault, down on the west and separating the gently dipping and steeply dipping beds, is associated with dolerite intrusion. The structure suggested by the increasing dips and the fault could be the synclinal flexure of an east-facing monocline cut by an antithetic fault. This structure lies 50 miles south of a west-facing monocline at Mt. Weeks and Cranfield Peak. It could be an extension of the Mt. Weeks monocline with a point of rotation between Coalsack Bluff and Cranfield Peak. It could also be part of an en echelon fault system or a graben.

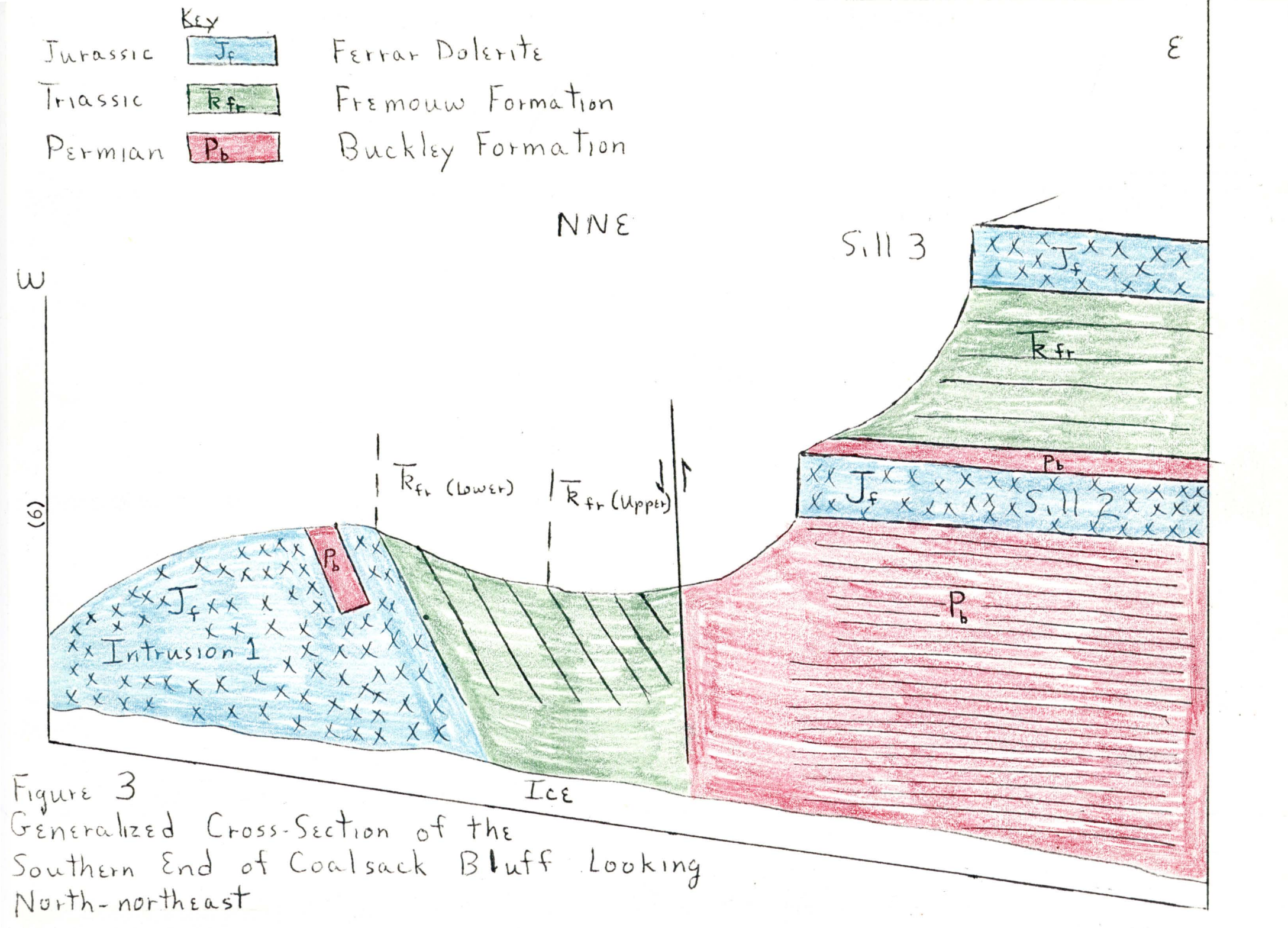

Figure 3
Generalized Cross-Section of the Southern End of Coalsack Bluff Looking North-northeast

Age Determination

Method

The method used to date the rock samples is based on the branched decay of potassium 40 (^{40}K) to argon 40 (^{40}Ar) and calcium 40 (^{40}Ca). The decay of ^{40}K to ^{40}Ar, the basis for K-Ar work, takes place by electron capture. An electron, usually from the K-shell, is captured by the nucleus, where it interacts with a proton to create a neutron. Decay of ^{40}K to ^{40}Ca takes place by the emission of a beta-minus particle.

The general formula for radioactive decay expressed in terms of present-day amounts of parent and daughter atoms is

$$D^* = N(e^{\lambda t}-1), \tag{1}$$

where D is the number of radiogenic daughter atoms, N is the number of parent atoms, t is the time since formation, and is the decay constant (the probability that an atom will decay in unit time). In terms of the branched decay of ^{40}K, equation (1) can be written

$$D_1^* + D_2^* = N(e^{(\lambda_1+\lambda_2)t}-1), \text{ or,} \tag{2}$$

$$^{40}Ar_{rad} + {}^{40}Ca_{rad} = {}^{40}K(e^{(\lambda_1+\lambda_2)t}-1), \tag{3}$$

where λ_1 and λ_2 are the decay constants for the ^{40}Ar and ^{40}Ca branches. The decay constants in use today are

$$\lambda_1 = 0.585 \times 10^{-10}\,yr^{-1} \text{ and} \tag{4}$$

$$\lambda_2 = 4.72 \times 10^{-10}\,yr^{-1}. \tag{5}$$

$$\text{The total decay constant, } \lambda_1 + \lambda_2 = \lambda = 5.305 \times 10^{-10}\,yr^{-1}. \tag{6}$$

The ratio of ^{40}Ar to ^{40}Ca produced by the decay of ^{40}K is the branching ratio, R, where

$$R = \frac{\lambda_1}{\lambda_2} = 0.1239, \text{ or,} \tag{7}$$

because this is the ratio of the daughters,

$$R = \frac{D_1}{D_2}. \tag{8}$$

The half-life of ^{40}K is related to by the equation

$$t_{\frac{1}{2}} = \frac{\ln 2}{\lambda} = \frac{0.693}{\lambda_1 + \lambda_2} = 1.31 \times 10^9 \text{yrs.} \quad (9)$$

Using the final age equation (derived in Appendix A), where

$$t = \frac{1}{\lambda} \ln\left[1 + \frac{D_1(1+\frac{1}{R})}{P}\right], \quad (10)$$

and substituting ^{40}K and $^{40}Ar^*$ (radiogenic) and the values for R and λ, we have

$$t = 1.885 \times 10^9 \ln\left[1 + \frac{9.071\ ^{40}Ar^*}{^{40}K}\right] \text{years}, \quad (11)$$

where $^{40}Ar^*$ and ^{40}K are expressed in moles or atoms.

Several assumptions made in the use of this model are:

1) that the system has remained closed since the time of formation; any loss or gain of potassium or argon will result in an incorrect age;
2) that no original daughter was present at the time of formation;
3) that the decay constants and isotopic abundances are accurately known;
4) that the age of the material represents the true age of formation;
5) and that the properties of the isotopes of an element are equal, i. e., there is no isotopic fractionation.

Potassium measurement

A small sample (0.1 gm.) of the powdered rock is dissolved in acid and heated. Excess acids, silicon, and fluorine are driven off by evaporation; other unwanted elements are precipitated as insoluble carbonates or sulfates and filtered out, leaving a final sulfate solution that contains the alkalai metals and magnesium. Great care must be exercised in preparing the solutions. Errors in measurement can result from contamination by improper handling, loss of sample, or from incorrect readings on the flame photometer. Two specimens of each sample are run and the difference between the two percentages must be less than 2% or another pair of analyses is made.

The flame photometer works on the principle that all atoms emit radiation

when excited above "ground state". The radiation spectrum is unique for each element and the intensity of the radiation is proportional to the amount of the element present. The unknown solution is bracketed between two solutions of known potassium concentration (all three contain equal concentrations of lithium) and readings from the three are compared. The readings of the unknown should fall between the readings of the two known solutions, permitting the calculation of the potassium concentration by linear interpolation.

The flame photometer is represented in Figure 4. The solution is atomized, mixed with propane gas, and fed into the burner flame. The radiation travels through a converging lens then through a potassium filter. The beam is recorded in a photomultiplier tube; the resulting current generated is fed into a differential amplifier and is read on a scale. The averages of the readings for the unknown solutions and the standards are used in the calculation of the percentage of potassium. The results appear in Table 1.

Argon measurement

Isotope dilution is a sensitive analytical means of determining the amount of radiogenic argon 40. A whole rock sample is placed in a molybdenum crucible, hung in a glass bottle at one end of a high-vacuum extraction line (Fig. 5). An induction furnace creates a radio frequency alternating current in the crucible, producing heat which melts the sample. All gases are allowed to boil off into the first half of the extraction line and collected in a charcoal finger immersed in liquid nitrogen. During fusion, a spike of argon, whose isotopic abundances are known, is admitted into the line. After cooling of the sample, the charcoal finger is warmed to room temperature; hydrogen is oxidized to H_2O and hydrocarbons are oxidized or ignited by a copper-copper oxide furnace connected to the line. Water is absorbed by the synthetic molecular dessicant. Next the gas is transferred to the second half of the line, using another finger of charcoal immersed in liquid nitrogen. The high-

Figure 4. Flame Photometer

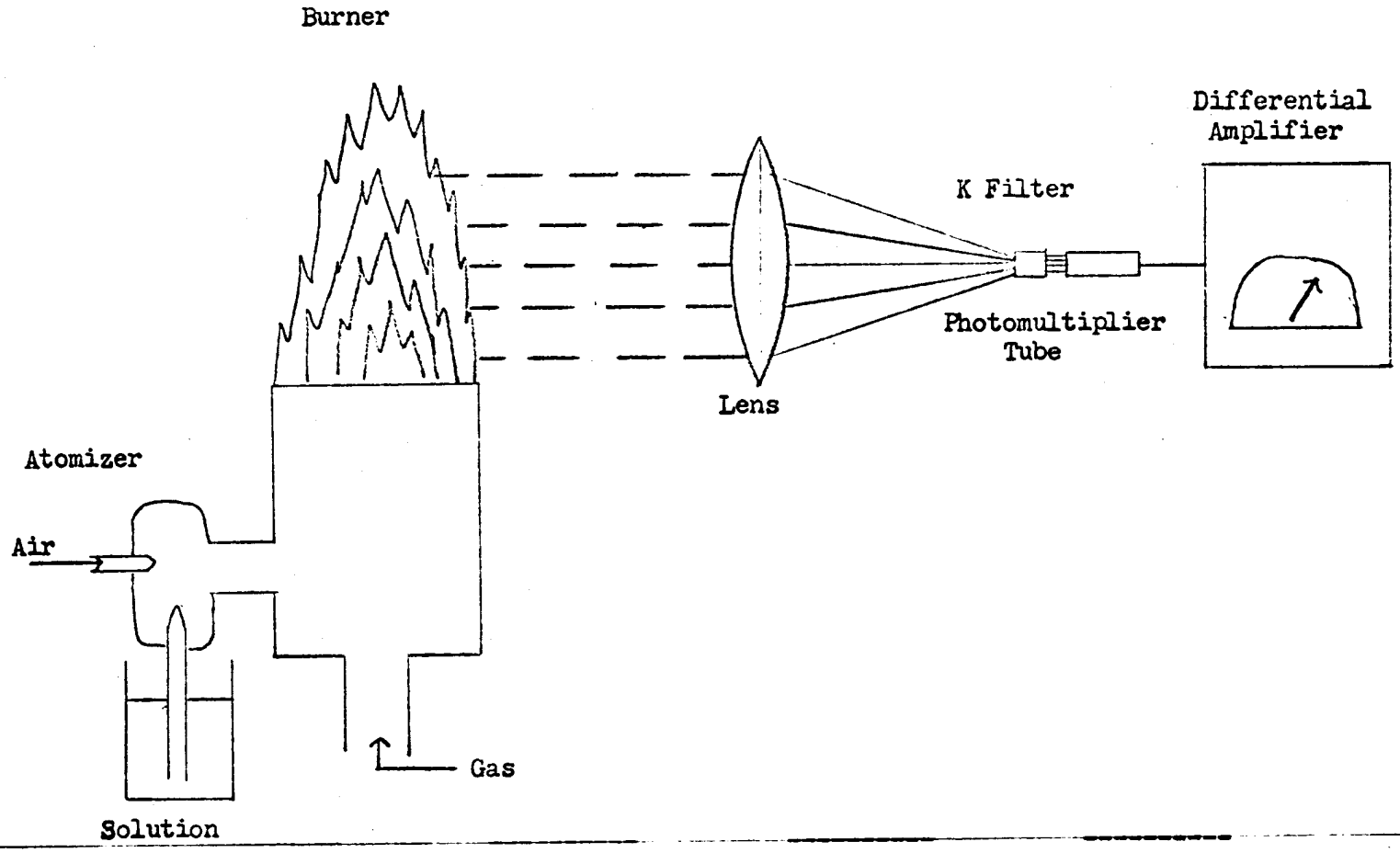

Figure 5. High-vacuum Extraction Line

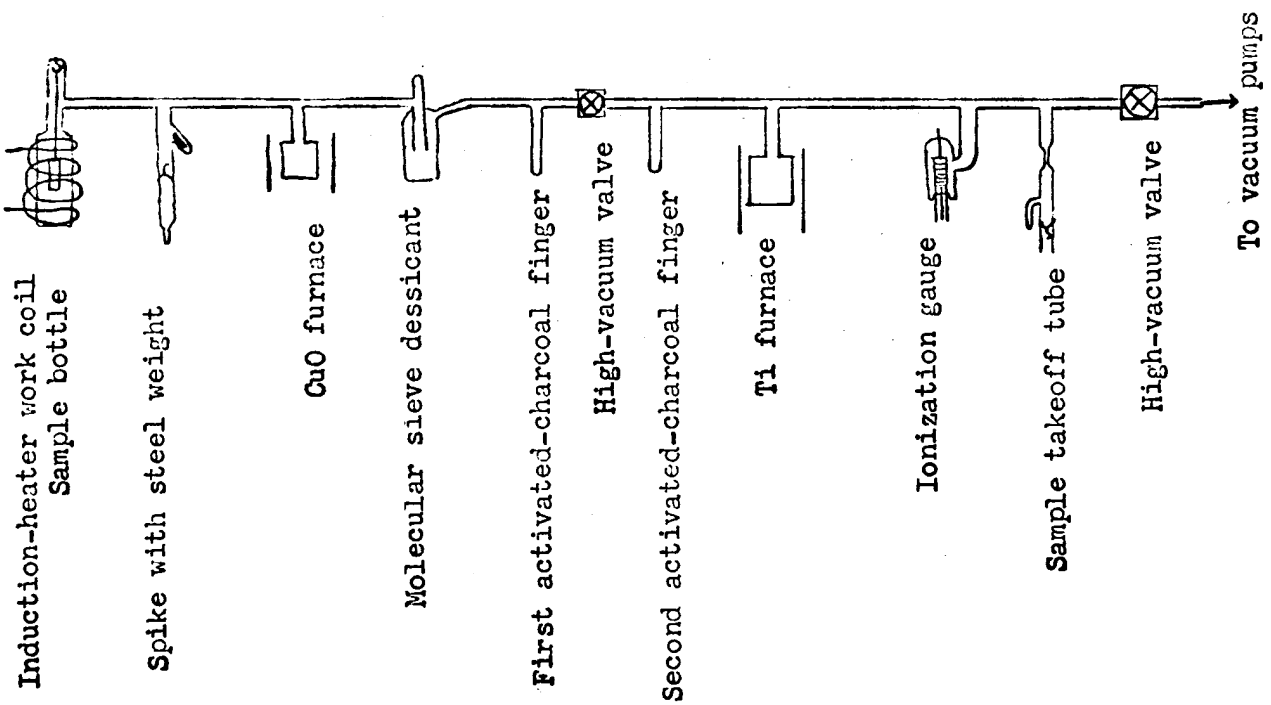

vacuum valve is closed, sealing the gas in the second half of the line, the finger warmed, and the gas is admitted to a titanium furnace at 800 C. The titanium metal adsorbs most of the reactive gases (O_2, N_2, etc.). After cooling, the remaining gas, which is almost pure argon, is collected in the small charcoal finger of the sample takeoff tube. The tube is removed and attached to the manifold system of the mass spectrometer.

The mass spectrometer (Fig. 6) works on the principle that the path of an ionized particle accelerated down a vacuum tube will be deflected when passing through a magnetic field. The amount of deflection will be directly proportional to the charge-to-mass ratio (e/M) of the particle and the strength of the magnetic field. The argon sample is allowed to enter a high-vacuum ion source (Fig. 6) and is ionized by electron bombardment. The ions are collimated and accelerated down the tube and their path is bent by the variable magnetic field of the mass analyzer. Ions whose paths are deflected so as to continue down the tube are collected in an ion detector (Faraday cup), creating a current in the measuring device. The amount of current is directly proportional to the amount of charged particles striking the cup. By using different magnet currents in the mass analyzer, ions of a certain e/M can be deflected into the detector, the result being that the ratios of the different isotopes of argon can be measured.

As each mass is analyzed by varying the magnet current and peak heights of each mass are recorded on a chart recorder. The peak heights, which are proportional to ion currents, are later measured and the 38/36 and 40/38 ratios are plotted versus time. These values form two lines which, when extrapolated back to time zero (the time of gas admittance into the mass spectrometer), give the original ratios of argon isotopes in the gas sample, which are corrected for scale differences resulting from the different ion currents. These ratios are used in the isotope dilution formula to determine the amount of

Figure 6. Mass Spectrometer

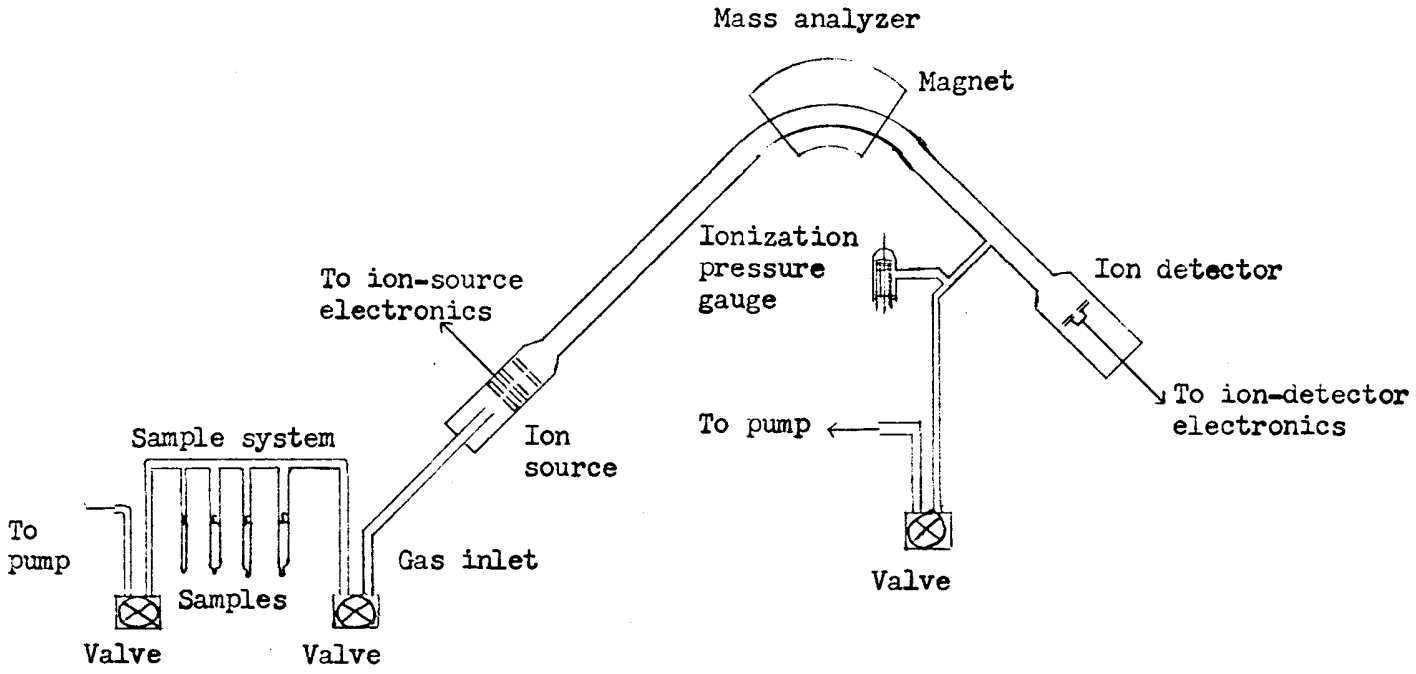

radiogenic argon 40. (Derivation of the isotope dilution formula is shown in Appendix B.) The results of the analysis and the age determinations are shown in Table 1.

Samples CB1-2 and CB1-6 were collected from the lower sill (Fig. 3). The samples are diabase because of mineral content and mineral orientation. Lathes of plagioclase surrounding shapeless masses of pyroxene (diabasic texture) are present in CB1-2 and prominent in CB1-6. CB1-6 contained some carbonate, but any alteration present produced no apparent effect on their ages. These specimens were little altered and had high potassium and radiogenic argon concentrations which lead to an excellent age determination.

Samples CB2-5 and CB3-3 were collected from sills 2 and 3 respectively (Fig. 3). Both exhibited diabasic texture but,not as prominently as that in the samples from sill 1. Plagioclase was prominent in CB2-5 and the pyroxene was somewhat altered. In CB3-3 the pyroxene was much altered. Deuteric alteration was present in both CB2-5 and CB3-3 but had little effect on their ages as is shown by the close agreement. The difference in potassium content between the two samples could be the result of differentiation during cooling.

Table 1

Sample	Intrusion	% K^+	% K_2O	moles ^{40}Ar/gm ($\times 10^{-10}$)	$^{40}Ar/^{40}K$ ($\times 10^{-2}$)	% rad ^{40}Ar	Age* (10^6 yrs)
CB1-2	lower	0.8007	0.965	2.5190	1.0337	56.6	168.9 ± 2.5
CB1-6	lower	0.8423	1.015	2.6047	1.0161	85.8	166.1 ± 2.0
CB2-5	middle	0.4118	0.496	1.3678	1.0914	20.7	177.9 ± 4.5
CB3-3	upper	0.8656	1.043	2.8792	1.0930	78.5	178.1 ± 3.0

* Ages are reported to 4 significant figures for internal comparison only. Error estimates are based on Ohio State University reproducibility (= ± 2 %, Fleck, 1970, personal communication) modified by % radiogenic argon 40. These ages were calculated using $\lambda_1 = 5.85 \times 10^{-11} yr^{-1}$, $\lambda_2 = 4.72 \times 10^{-10} yr^{-1}$, and $\frac{\lambda_1}{\lambda_2} = 0.1239$.

Paleomegnetism and Analysis of Data

The earth's magnetic field may be described in terms of three components: a relatively small component due to processes occurring above the earth's surface; a dipole component equivalent to the field of a magnetic dipole located at the center of the earth and inclined 11.5 degrees from the axis of rotation; and a nondipole component, which would remain if the externally produced field and the dipole field were removed. These three components are easily separated if the earth's magnetic field is represented by means of spherical harmonics.

The nondipole component is described by the higher order harmonics, and the dipole component is completely described by the first order harmonic. The dipole that best fits the irregular field of the earth is one that is inclined 11.5 degrees to the axis of rotation and which intersects the earth's surface at 78.5 degrees North Latitude and 69 degrees West Longitude. This point is, by definition, the geomagnetic pole. Theoretical considerations and paleomagnetic results suggest that this pole has not remained stationary; however, there is no direct evidence that it has moved. In the late nineteenth century, when adequate data became available, an accurate pole position was determined, and since that time, the pole has remained within 0.5 degrees of its present position.

A comparatively irregular, rapidly changing, nondipole field is superimposed on the stable dipole field. This nondipole field consists of irregularly distributed regions of high and low intensity ranging in diameter from 25 degrees to 100 degrees. Like centers of cyclonic activity in the atmosphere, these regions wax and wane with a life, suggested by present rates of change, of about 100 years. These surface features exhibit a movement that is not entirely random, but shows a systematic westward drift of about one-fifth degree of longitude per year.

As a molten rock cools, these external fields produce certain effects in the rock. In each grain of magnetic material there exists one or more magnetic

domains. The intensity of magnetization per unit volume is the same in all domains of the same material. This quantity decreases with an increase in temperature and vanishes at the Curie temperature. In the absence of an external magnetic field the direction of magnetization will lie along one of several preferred axes. The directions of these axes and the heights of the magnetic barriers that separate them are determined by the shape of the grain, the crystalline anisotropy, or both. In an applied field of increasing intensity, the direction of magnetization in the grain is pulled away from the preferred axis toward the field direction. If the energy of the applied field is insufficient to surpass the energy barriers, the direction of magnetization will return to the preferred orientation when the field is removed. This is termed, by definition, an induced magnetization.

If the applied field is increased above a certain value termed the coercive force, the direction of magnetization in a grain crosses over a magnetic energy barrier, and when the field is removed the magnetic vector lines up along a new direction nearly parallel to the applied field. This irreversible magnetization is a remnant or permanent magnetization.

The process of thermo-remnant magnetization (TRM) is very important in paleomagnetic studies. During cooling in the earth's magnetic field, a rock begins to develop a spontaneous magnetization at the Curie temperature and a preferred alignment of domains parallel to the field. Not all of this TRM is acquired at the Curie temperature, but rather over an interval ranging some tens of degrees below the Curie temperature. The orientation has a certain declination and inclination determined by the rock's position relative to the geomagnetic pole. The declination and inclination are measurable and are used in the calculation of the paleogeomagnetic pole.

It is convenient to represent the paleomagnetic data in terms of the geocentric dipole that would produce the measured field direction. To do this one specifies the geographic co-ordinates of the geomagnetic pole that corresponds

to the orientation of the inferred dipole. Given the paleomagnetically determined declination and inclination of the field in the oriented rock sample, the position of the geomagnetic pole corresponding to this observed direction is given by the following relations:

$$\cot p = \tfrac{1}{2} \tan I \qquad (1)$$

$$\sin \Theta' = \sin \Theta \cos p + \cos \Theta \sin p \cos D \quad \text{(the dipole formula)} \qquad (2)$$

$$\sin(\phi' - \phi) = (\sin D \sin p)/\cos \Theta' \qquad (3)$$

where p is the angle between the present meridian and the paleomeridian; Θ' and ϕ' are the latitude and longitude of the paleogeomagnetic pole; Θ and ϕ are the latitude and longitude of the sampling site; and D and I are the declination and inclination of the field in the sample. The pole thus found is termed a virtual geomagnetic pole. The data for the three dolerite intrusions on Coalsack Bluff are summarized in Table 2.

Table 2

Sample Number	Location	D	I	Virtual Pole
CB1-2, CB1-6	Lower sill	238.4	-77.4	64 36' S, 143 44' W
CB2-5	Middle sill	353.2	-76.4	46 24' S, 139 2' W
CB3-3	Upper sill.	244.4	-66.6	46 12' S, 139 30' W

Conclusions

Pertinent paleomagnetic data and ages are summarized in Table 3. CB1-2, CB1-6, CB2-5, and CB3-3, are hereafter reffered to as intrusions 1, 2, and 3 respectively.

Table 3

Intrusion	Virtual Pole	Age (X 10^6 yrs.)
1	64 36' S, 143 44' W	167.5 ± 4.0
2	46 24' S, 139 2' W	177.9 ± 4.5
3	46 12' S, 139 30' W	178.1 ± 3.0

Folding predates intrusion of 2 and 3 because these intrusions are discordant and are absent from the section of steeply dipping strata. The faulting is either contemporaneous with folding or postdates it. Intrusion 1 was implaced after tilting or monoclinal folding occurred because it is concordant with strata whose attitude is at least 50 degrees different from intrusions 2 and 3, but has a pole position within 20 degrees of that for intrusions 2 and 3.

The structure seems to be an east-facing monocline cut by an antithetic fault. The monoclinal folding occurred before 178 million years ago. Whether faulting occurred contemporaneous with folding or postdates it is unknown because any contact between the fault and intrusions 2 and 3 has been removed by erosion. Intrusion 1 parallels the fault and it appears that the fault zone was used as a zone of weakness along which the intrusion travelled. Since intrusion 1 is concordant, it probably is contemporaneous with or postdates the fault.

Paleomagnetically, the intrusions are quite interesting. The older intrusions, 2 and 3, show a virtual pole different from that of intrusion 1. If these poles are plotted on Figure 7, they show good agreement with the polar wandering curve of K. M. Creer. (Creer shows no data other than the wandering curve, but these data seem to support his curve.) The changes in the pole position may correspond

Figure 7

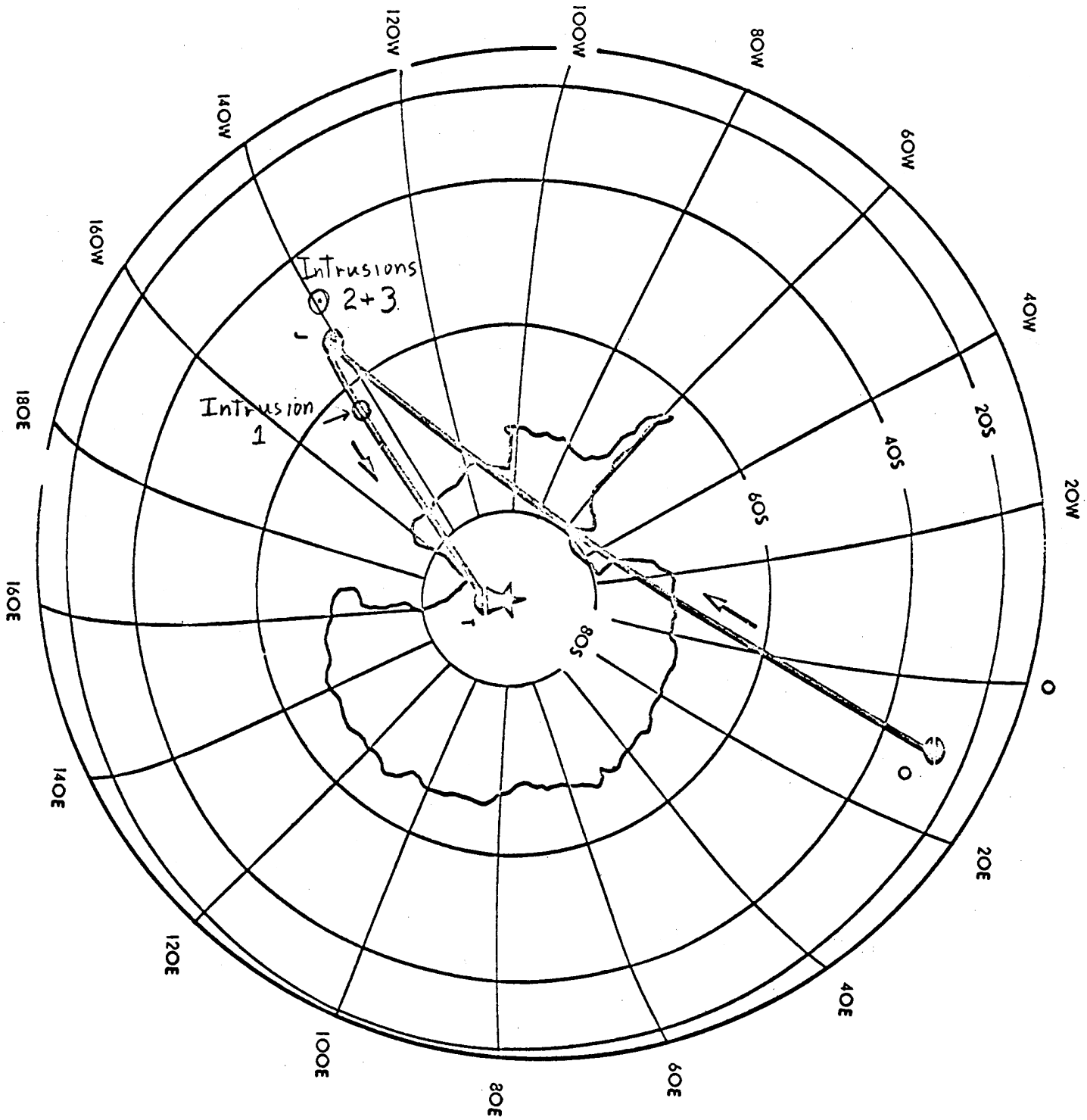
Intrusions
2+3
Intrusion
1
120W
100W
80W
60W
40W
20W
0
20E
40E
60E
80E
100E
120E
140E
160E
180E
160W
140W
20S
40S
60S
80S

to the difference in ages, and, assuming no rotation since intrusion, may indicate a drift toward the present-day pole.

Personal communication with Dr. Alan Nairn has raised the possibility of secular variation affecting the position of the pole. Secular variation is the change in the geomagnetic field in any one place from year to year. This change is one of direction, and the range of the variation can be from ten to twenty degrees on either side of the average. Changes occurring in the southern hemisphere are rapid and show a westward drift of the center of most rapid change of 0.32 ± 0.07 degrees of longitude per year (Bullard and others, 1950). An age difference of 10^4 years (preferably 10^5 years) is usually adequate to counteract the effects of secular variation. Therefore, the minimum age difference between the two intrusions (5×10^5 years) may be sufficient to rule out a pole change due to secular variation.

If secular variation can be ruled out, these poles and their respective dates are further proof of Antarctica's drift. Antarctica appears to have moved meridianally during the Early Jurassic at a rate of approximately 10 to 18 cm/yr. This drift rate is somewhat faster than that for the Atlantic, 5 cm/yr., but is possible. The direction of drift is consistent with models moving the continent to its present location. The drift direction and position at the time of intrusions 2 and 3 fit a model suggested by Dietz and Holden, 1970. These dates are significant because they show a drift direction and a rate of drift for two closely spaced time intervals within the same geologic period. If the time interval was in fact greater, the drift rate would be slower and more in agreement with present drift rates.

Appendix A

Radioactive decay is a statistical process in which the number of atoms that disintegrate per unit time, $-dP/dt$, is proportional to the number of atoms present, P. Thus

$$-\frac{dP}{dt} = \lambda P. \tag{1}$$

Integrating between $P = P_o$ at $t = t_o$ and $P = P$ at $t = t$, equation (1) becomes

$$\int_{P_o}^{P} \frac{dP}{P} = -\int_{t_o}^{t} \lambda t, \tag{2}$$

$$\ln \frac{P}{P_o} = -\lambda t, \tag{3}$$

$$P = P_o e^{-\lambda t}, \tag{4}$$

which is the basic radioactive decay formula.

If no parent or daughter atoms are gained or lost, the rate of decrease in the number of parent nuclides must be equal to the rate of increase in the number of daughter nuclides, D, at any time, t:

$$\frac{dD}{dt} = -\frac{dP}{dt}. \tag{5}$$

At any time, t,

$$P_o = P + D. \tag{6}$$

Substituting equation (6) into equation (4),

$$D = P(e^{\lambda t} - 1). \tag{7}$$

For K-Ar branching decay, equation (7) can be written

$$D_1 + D_2 = P(e^{(\lambda_1 + \lambda_2)t} - 1), \tag{8}$$

where D_1 and D_2 are the two daughter nuclides and λ_1 and λ_2 are their decay constants. Solving equation (8) for t we get

$$t = \frac{1}{\lambda_1 + \lambda_2} \ln\left[\frac{P + D_1 + D_2}{P}\right], \text{ or} \tag{9}$$

$$t = \frac{1}{\lambda_1 + \lambda_2} \ln\left(1 + \frac{D_1 + D_2}{P}\right). \tag{10}$$

The ratio of the two daughters is defined as the Branching Ratio, R, where

$$R = \frac{D_1}{D_2}, \text{ and} \tag{11}$$

$$D_2 = \frac{D_1}{R}. \tag{12}$$

Using $\lambda = \lambda_1 + \lambda_2$ and substituting for D_2,

$$t = \frac{1}{\lambda} \ln 1 + \left[\frac{D_1 (1 + \frac{1}{R})}{P} \right], \tag{13}$$

which is the general age equation for K-Ar work.

Appendix B

Derivation of Isotope Dilution Formula

Definitions

Ar^{40}_{rad} = atoms of radiogenic Ar^{40} in sample

Ar^{i}_{T} = atoms of isotope i in tracer (spike)

Ar^{i}_{A} = atoms of isotope i in atmospheric contaminant

Ar^{i}_{M} = atoms of isotope i in mixture

The subscripts also apply to the isotope ratios.

Given the following equations:

(a) $Ar^{40}_{M} = Ar^{40}_{rad} + Ar^{40}_{T} + Ar^{40}_{A}$,

(b) $Ar^{38}_{M} = Ar^{38}_{T} + Ar^{38}_{A}$,

(c) $Ar^{36}_{M} = Ar^{36}_{T} + Ar^{36}_{A}$,

we rewrite (a) and (c):

(d) $Ar^{40}_{M} = Ar^{40}_{rad} + (Ar^{40}/Ar^{38})_{T} Ar^{38}_{T} + (Ar^{40}/Ar^{38})_{A} Ar^{38}_{A}$.

(e) $Ar^{36}_{M} = (Ar^{36}/Ar^{38})_{T} Ar^{38}_{T} + (Ar^{36}/Ar^{38})_{A} Ar^{38}_{A}$.

Divide (b) by (e) and solve for Ar^{38}_{A}:

(f) $$Ar^{38}_{A} = Ar^{38}_{T}\left[\frac{1-(Ar^{38}/Ar^{36})_{M}(Ar^{36}/Ar^{38})_{T}}{(Ar^{38}/Ar^{36})_{M}(Ar^{36}/Ar^{38})_{A}-1}\right]$$

Divide (d) by (b) and solve for Ar^{40}_{rad}:

(g) $$Ar^{40}_{rad} = Ar^{38}_{Tad}(Ar^{40}/Ar^{38})_{M} - Ar^{38}_{T}(Ar^{40}/Ar^{38})_{T} - Ar^{38}_{A}\left[(Ar^{40}/Ar^{38})_{A} - (Ar^{40}/Ar^{38})_{M}\right].$$

Substitute (f) into (g) and simplify:

$$Ar^{40}_{rad} = Ar^{38}_{T}\left\{(Ar^{40}/Ar^{38})_{M}-(Ar^{40}/Ar^{38})_{T} - \left[\frac{1-(Ar^{38}/Ar^{36})_{M}(Ar^{36}/Ar^{38})_{T}}{(Ar^{38}/Ar^{36})_{M}(Ar^{36}/Ar^{38})_{A}-1}\right]\left[(Ar^{40}/Ar^{38})_{A}-(Ar^{40}/Ar^{38})_{M}\right]\right.,$$

which is the isotope dilution formula.

Bibliography

Blundell, D. J., Paleomagnetism of the Dolerite Intrusions, In Transantarctic Expedition 1955-1958, Scientific Reports, No. 8.

Collinson, D. W., Creer, K. M., and Runcorn, S. K., eds., Methods in paleomagnetism, In Developments in Solid Earth Geophysics, vol. 3, 1967.

Collinson, J. W. and Elliot, D. H., Geology of Coalsack Bluff, Antarctica's First Major Triassic Vertebrate Locality, in preparation.

Cox, A., and Doell, R. R., Review of Paleomagnetism, G. S. A. Bull., June, 1960, vol. 71, p. 645-768.

Creer, K. M., Review and Interpretation of Paleomagnetic Data From the Gondwanic Continents.

Dalrymple, G. B. and Lanphere, M. A., Potassium-Argon Dating, 1969, W. H. Freeman & Company.

Dietz, R. S. and Holden, J. C., The Breakup of Pangea, Scientific American, October, 1970.

Elliot, D. H., Collinson, J. W., and Powell, J. S., Stratigraphy of Triassic Tetrapod-Bearing Beds of Antarctica, Proceedings of the Second I. U. G. S. Symposium on the Stratigraphy and Paleontology of the Gondwana System.

Hamilton, E. I., Applied Geochronology, 1965, Academic Press, London, p. 47-80.

Irving, E., Paleomagnetism and Its Application to Geological and Geophysical Problems, Wiley & Sons 1964.